Crystal-field analysis of the spectroscopic characteristics and magnetic properties of Tm^{3+} in $LiYF_4$ crystal

1997 J. Phys.: Condens. Matter 9 4197

(http://iopscience.iop.org/0953-8984/9/20/018)

J. Phys.: Condens. Matter **9** (1997) 4197–4210. Printed in the UK PII: S0953-8984(97)80617-0

Crystal-field analysis of the spectroscopic characteristics and magnetic properties of Tm^{3+} in $LiYF_4$ crystal

Chen Xueyuan† and Luo Zundu†‡

† Fujian Institute of Research on the Structure of Matter, Chinese Academy of Sciences, Fuzhou, Fujian, 350002, People's Republic of China

‡ China Centre of Advanced Science and Technology (World Laboratory), PO Box 8730, Beijing 100080, People's Republic of China

Received 3 January 1997

Abstract. On the basis of the analysis of a group-chain scheme and with the use of the constraint condition determined by the ratios of crystal-field parameters calculated using the point-charge model, a crystal-field-level fitting has been carried out for Tm^{3+}:$LiYF_4$, in which the Tm^{3+} ions are assumed to occupy positions with point symmetry D_{2d}. The RMS value of the energy-level fitting is 11.4 cm^{-1}. The wavefunctions obtained were used in the study of the magnetic, thermal, and spectroscopic properties of the crystal. The calculated g-factors obey Karayianis's partial g-sum rule. The temperature dependences of the Schottky specific heat and magnetic susceptibility agree well with data published by others. The line shown by calculation to be the strongest is σ-polarized at 450.4 nm, which corresponds to blue upconversion lasing in the experiment. The method proposed turns out to be effective in the study of the spectroscopic and magnetic properties of localized centres in crystals.

1. Introduction

In recent years, there has been a revival of interest in obtaining solid-state blue and green lasers that can be pumped by available red or near-infrared semiconductor laser diodes. Triply ionized thulium in lithium yttrium fluoride (Tm^{3+}:$LiYF_4$) is an ideal upconversion material with good laser performance. Jenssen *et al* [1] and Dulick *et al* [2] have reported the energy levels of Tm^{3+}:$LiYF_4$, and assigned S_4 symmetry to the Tm^{3+}-ion substitutional site. The crystal-field (CF) parameters of Tm^{3+}:$LiYF_4$ were used to find the temperature variations of the Schottky specific heat and paramagnetic susceptibility by Kumar *et al* [3]. Blue upconversion lasing in Tm^{3+}:$LiYF_4$ at 450.2 and 483.0 nm has been well documented [4–7]. It is important to study the detailed structure of the energy levels in order to improve the laser efficiency, and to study the upconversion dynamics.

In previous work, the energy levels and spectroscopic properties of NAB, NYAB [8], Nd^{3+}:YVO_4 [9], and Er^{3+}:$LiYF_4$ [10] have been investigated. The same method, namely that of a group-chain scheme plus a constraint condition determined by the ratios of CF parameters, can also be used to study the energy levels of Tm^{3+}:$LiYF_4$. Utilizing the fitting wavefunctions, we can calculate the spectroscopic splitting g-factors, Schottky specific heat, paramagnetic susceptibility, and relative line-to-line intensities between Stark sublevels. The results will be compared with data published by others.

0953-8984/97/204197+14$19.50

2. The group-chain scheme analysis

The actual site symmetry of Tm^{3+} in $LiYF_4$ is S_4, approximately D_{2d}. The lowering of the symmetry from D_{2d} to S_4 is caused by a slight distortion of the dodecahedron of Tm^{3+} ions. The distortion angle $\Delta\varphi$ is 2.29° [11]. As the angle is small, the D_{2d} symmetry remains a good approximation for the S_4 symmetry. This is also supported by the zero value of $\mathrm{Im}\, B_{64}$ in table 1 of reference [2].

Consider the group chain $O_3 \supset O_h \supset T_d \supset D_{2d}$; the detailed CF Hamiltonian can be expressed in Butler's notation:

$$H_{cf} = C^{2^+}_{2^+2} b^{2^+}_{2^+2} + C^{4^+}_{0^+0} b^{4^+}_{0^+0} + C^{4^+}_{2^+2} b^{4^+}_{2^+2} + C^{6^+}_{0^+0} b^{6^+}_{0^+0} + C^{6^+}_{2^+2} b^{6^+}_{2^+2}. \tag{1}$$

Here the $b^k_{\mu\nu}$ are the basis functions of the group chain $O_3 \supset O_h \supset T_d \supset D_{2d}$, and are identical to the $|k\mu\nu 0\rangle$ in [12]; the $C^k_{\mu\nu}$ are the coefficients of the expansion of H_{cf} in terms of these bases; and the symbol '+' denotes that the representation belongs to the even-parity representation. Because all of the basis functions belong to the 0 representation of D_{2d} in the calculation concerned, the index 0 has been omitted for the D_{2d} group.

The wavefunctions of all of the Stark levels can be expressed as

$$\Psi = \sum_{a a_1 a_2 a_3} C^a_{a_1 a_2 a_3} |a a_1 a_2 a_3\rangle. \tag{2}$$

The matrix elements of the CF Hamiltonian in the group-chain scheme can be calculated by means of the Wigner–Eckart theorem and the factorization lemma for the $3jm$-factors:

$$\begin{aligned}\langle a a_1 a_2 a_3 | H_{cf} | b b_1 b_2 b_3\rangle &= \sum_{k\mu\nu} C^k_{\mu\nu} \begin{pmatrix} a \\ a_1 \end{pmatrix} \begin{pmatrix} a_1 \\ a_2 \end{pmatrix} \begin{pmatrix} a_2 \\ a_3 \end{pmatrix} \sum_{r r_1 r_2 r_3} \begin{pmatrix} a^* & k & b \\ a_1^* & \mu & b_1 \end{pmatrix}_{r r_1} \begin{pmatrix} a_1^* & \mu & b_1 \\ a_2^* & \nu & b_2 \end{pmatrix}_{r_1 r_2} \\ &\quad \times \begin{pmatrix} a_2^* & \nu & b_2 \\ a_3^* & 0 & b_3 \end{pmatrix}_{r_2 r_3} \langle a || b^k || b\rangle \end{aligned} \tag{3}$$

$$\langle a || b^k || b\rangle = \langle \mathrm{f}^n S L a || U^{(k)} || \mathrm{f}^n S' L' b\rangle \langle 4\mathrm{f} || C^{(k)} || 4\mathrm{f}.\rangle \tag{4}$$

The reduced matrix elements (RME) $\langle \mathrm{f}^n SLa || U^{(k)} || \mathrm{f}^n S'L'b\rangle$ were calculated under the intermediate-coupling approximation [13]. All of the $2jm$- and $3jm$-factors can be found from [12]. The energy-level fitting is performed in two steps instead of by diagonalizing a combined spin–orbit and CF Hamiltonian. First, free-ion wavefunctions in a terms of a Russell–Saunders basis of J-states are obtained by diagonalizing a Hamiltonian containing the Coulomb and spin–orbit interactions, and thus we can compute the RME of $U^{(k)}$ ($k = 2, 4, 6$) connecting all of the intermediately coupled wavefunctions. Second, matrices (such as the 10×10 matrix of $^3H_6$, and the 7×7 matrix of $^3F_4$) representing the CF interaction are diagonalized simultaneously for $^{2S+1}L_J$ states for which data on experimental energy levels exist, and the CF parameters are determined in a least-squares fit to the data. Here we assume that the centres of gravity of the J-multiplets are invariant even in the CF interaction, because the effect of J-mixing in Tm^{3+}:$LiYF_4$ is negligible.

On the basis of the group–subgroup chain $O_3 \supset O_h \supset T_d \supset D_{2d}$, the wavefunctions of the $4f^{12}$ configuration in Tm^{3+} at the D_{2d} symmetry position are expressed as linear combinations of the bases $|\mathrm{f}^n SLJ\mu\nu\xi\rangle$ in the group-chain scheme, where μ, ν, and ξ are the irreducible representations of O_h, T_d, and D_{2d} respectively. From equation (3), the detailed matrix elements of all of the terms can be obtained. The conventional CF parameters are calculated using the simple point-charge model. Consider the shielding factors of the $5s^25p^6$ shells and the scaling parameters of the bare Hartree–Fock wavefunction [14]:

$$B_{nm} = \rho_n A_{nm} \tag{5}$$

with, for Tm^{3+},

$$\rho_2 = 0.1722 \qquad \rho_4 = 0.4053 \qquad \rho_6 = 0.9649.$$

A_{nm} is the result of the lattice summation. Using the conversion relationship of the conventional CF parameters and group-chain parameters [10], the initial values r_0, r_1 (the ratios of the same rank of group-chain parameters) can be obtained; these are listed in tables 1 and 2. Note that

$$\begin{aligned} r_0 &= C^{4+}_{2+2}/C^{4+}_{0+0} \\ r_1 &= C^{6+}_{2+2}/C^{6+}_{0+0}. \end{aligned} \tag{6}$$

The physical meaning of these constraint ratios in the fit has been discussed previously [10].

Table 1. The CF parameters B_{nm} for Tm^{3+}:$LiYF_4$.

B_{20}	B_{40}	B_{44}	B_{60}	B_{64}	Obtained from:
364.98	−618.22	1127.13	−96.16	317.94	Point-charge model
321.86	−638.51	888.33	−150.33	612.99	[2]
322.58	−625.98	906.73	−63.05	600.19	Fitting results

Table 2. Group-chain parameters, and constraint ratios.

C^{2+}_{2+2}	C^{4+}_{0+0}	C^{4+}_{2+2}	C^{6+}_{0+0}	C^{6+}_{2+2}	r_0	r_1	Obtained from:
−364.98	556.76	−1616.50	454.59	69.02	−2.9034	0.1518	Point-charge model
−321.86	323.26	−1371.66	864.06	165.87	−4.2432	0.1920	[2]
−322.58	349.63	−1383.45	816.27	241.12	−3.9569	0.2954	Fitting results

On using the ratios listed in table 2 as constraints in the least-squares fit, only one minimum was obtained. A further step in the fit is that of adjusting the ratios to minimize the RMS deviation of the energy levels. In table 2, comparisons of the initial and final k-even parameters $C^k_{\mu\nu}$ (cm^{-1}) and the corresponding ratios are given. The experimental and fitting energy levels are compared in table 3. The group attributes of Stark sublevels are also shown. 51 levels with the greatest experimental confidence are included in this fit:

$$\mathrm{RMS} = \sum_{i=1}^{51} (E_i^{\mathrm{exp}} - E_i^{\mathrm{theo}})^2/51 - 5. \tag{7}$$

The final fit give a RMS value of 11.4 cm^{-1}. By comparing this with the results of Jenssen [1] (RMS = 16.9 cm^{-1}) or Dulick *et al* [2] (RMS = 16 cm^{-1}), we can see that the calculated eigenvalues agree better with the experimental energy levels. The wavefunctions of the Stark levels of the total of 11 terms are normalized, and listed in the order of increasing energy in the appendix. In the case of the D_{2d} group, Butler's notation $0, \tilde{0}, 2, \tilde{2}$, and 1 corresponds to $\Gamma_1, \Gamma_2, \Gamma_3, \Gamma_4$, and Γ_5 respectively, in Bethe's notation. By using the wavefunctions given above, the g-factors of the Zeeman interaction can now be calculated.

3. The Zeeman interaction

Previously we have reported the theoretical calculation of the g-tensor of the ground and excited states in Er^{3+}:$LiYF_4$ [10], on the basis of a group-chain scheme analysis. The

Table 3. A comparison of the observed and calculated energy levels and g-factors of Tm^{3+} in $LiYF_4$ at 75 K.

		Energy (cm^{-1})		$g_\parallel$	
J-multiplet	Γ	Experimental[a]	Theoretical[b]	Theoretical[b]	Theoretical[c]
$^3H_6$	4	0	−6		
	5	30	26	−0.5477	−0.340
	1	56	57		
	3	270	273		
	4	305	298		
	2	319	336		
	5	334	347	11.6496	11.513
	1	372	393		
	5	407	387	−4.1028	−4.182
	3	419	414		
$^3F_4$	1	5599	5592		
	2	5756	5780		
	5	5757	5753	−0.2639	0.110
	4	5820	5805		
	3	5942	5939		
	1	5968	5977		
	5	5972	5972	−4.7355	−4.632
$^3H_5$	3	8284	8286		
	5	8300	8294	0.1338	0.193
	2	8319	8304		
	5	8501	8495	10.3258	10.121
	1	8519	8533		
	4	—	8554		
	5	—	8555	−4.2594	−4.144
	2	8535	8559		
$^3H_4$	4	12 599	12 593		
	1	12 624	12 609		
	5	12 643	12 638	0.0784	−0.087
	2	12 745	12 762		
	1	12 804	12 804		
	5	12 835	12 832	−3.2785	−3.677
	2	12 891	12 911		
$^3F_3$	5	14 520	14 517	−4.4064	−4.385
	4	14 549	14 549		
	5	14 594	14 599	0.0728	0.237
	3	—	14 602		
	2	14 597	14 586		

detailed derivation of the g-factor is also presented there. Here we can directly utilize the results. In Tm^{3+}:$LiYF_4$, only the Stark levels belonging to the Γ_5 representation of the D_{2d} group are doubly degenerate, and hence they might be split in a magnetic field. It can easily be proved that the doublet cannot be split in a magnetic field perpendicular to the crystal Z-axis; that is, all $g_\perp$-values are zero. Therefore only the opposite situation, where the magnetic field $\boldsymbol{H}$ is along the crystal Z-axis, needs to be considered. The calculation of the $g_\parallel$-values is similar to that for Er^{3+}:$LiYF_4$. The results are listed in table 3. We

Table 3. (Continued)

		Energy (cm^{-1})		$g_\parallel$	
J-multiplet	Γ	Experimental[a]	Theoretical[b]	Theoretical[b]	Theoretical[c]
$^3F_2$	3	15 094	15 097		
	5	15 203	15 198	1.3333	1.278
	4	—	15 238		
	1	15 275	15 276		
$^1G_4$	1	20 973	20 992		
	5	21 186	21 192	0.1819	0.381
	4	21 272	21 271		
	2	21 300	21 307		
	3	—	21 479		
	5	21 554	21 539	−4.1815	−4.219
	1	21 562	21 544		
$^1D_2$	4	27 961	27 958		
	3	27 991	27 999		
	5	28 053	28 057	2	2.243
	1	28 075	28 063		
$^1I_6$	3	—	34 561		
	5	34 729*	34 573	−2.0378	−2.160
	1	—	34 591		
	2	34 778	34 778		
	5	34 769*	34 877	6.3202	5.290
	4	—	34 997		
	1	34 999*	35 015		
	5	34 998*	35 023	1.7181	2.863
	3	—	35 193		
	4	—	35 196		
$^3P_1$	2	36 470	36 470		
	5	36 566	36 566	3	2.954
$^3P_2$	3	—	37 865		
	5	38 049	38 059	3	2.647
	4	—	38 167		
	1	38 241*	38 219		

[a]Dulick's spectra; see reference [2].
[b]Present results.
[c]Jenssen's parametrized fit; see [1].
*Levels excluded from the final fit.

believe that future experiments on $g_\parallel$-values of the excited states will support these results.

In order to confirm the reliability of the proposed method, we may sum all of the g-factors over levels belonging to the Γ_5 irreducible representation of a particular $^{2S+1}L_J$ state to check the partial g-sum rule [15]. The sums are compared with theoretical values and Jenssen's results in table 4. The better agreement between them shows that the group-chain scheme analysis, using one set of the CF parameter ratios as the constraint condition, is useful both in the study of the spectroscopic properties of laser crystals [8–10] and in the study of the properties of magnetic materials.

Table 4. A comparison of partial g-sums with theoretical values for the terms for Tm^{3+} in $LiYF_4$. (μ is the crystal quantum number.)

	Γ_5 (1)		
J	$\mu = 1$[a]	Tm^{3+}:$LiYF_4$[b]	Tm^{3+}:$LiYF_4$[c]
$^3H_6$	7.00	6.9991	6.991
$^3F_4$	−5.00	−4.9994	−4.522
$^3H_5$	6.20	6.2002	6.170
$^3H_4$	−3.20	−3.2001	−3.764
$^3F_3$	−4.33	−4.3336	−4.148
$^3F_2$	1.33	1.3333	1.278
$^1G_4$	−4.00	−3.9996	−3.838
$^1D_2$	2.00	2.0000	2.243
$^1I_6$	6.00	6.0005	5.993
$^3P_1$	3.00	3.0000	2.954
$^3P_2$	3.00	3.0000	2.647

[a]Theoretical values (reference [15]).
[b]Present results.
[c]Jenssen's results; see [1].

4. The Schottky specific heat and the magnetic susceptibility

Another two interesting phenomena caused by the CF splitting are the Schottky anomaly and the magnetic anisotropy. The mole Schottky specific heat (C_S) is calculated from the following equation:

$$C_S = \frac{Nk}{Z^2}\left[Z\sum_{i=1}^{n}\left(\frac{E_i^0}{kT}\right)^2 g_i \exp\left(-\frac{E_i^0}{kT}\right) - \left\{\sum_{i=1}^{n}\left(\frac{E_i^0}{kT}\right) g_i \exp\left(-\frac{E_i^0}{kT}\right)\right\}^2\right] \tag{8}$$

where E_i^0 is the zeroth-order energy eigenvalue of the ith level, g_i denotes the degree of degeneracy, and

$$Z = \sum_{i=1}^{n} g_i \exp(-E_i^0/kT).$$

The mole magnetic susceptibility χ is calculated from the Van Vleck formulation:

$$\chi = \frac{N}{Z}\sum_{i=1}^{n}\left[\frac{(E_i^1)^2}{kT} - 2E_i^2\right]\exp(-E_i^0/kT) \tag{9}$$

where E_i^1, E_i^2 are the first- and second-order perturbation energy eigenvalues corresponding to the magnetic field $\boldsymbol{H}$ parallel or perpendicular to the crystal z-axis:

$$E_i^1 = \mu_B\langle\psi_i|\boldsymbol{L} + 2\boldsymbol{S}|\psi_i\rangle \tag{10}$$

$$E_i^2 = \mu_B^2\sum_{j\neq i}\frac{|\langle\psi_i|\boldsymbol{L} + 2\boldsymbol{S}|\psi_j\rangle|^2}{E_i^0 - E_j^0} \tag{11}$$

where ψ_i is the wavefunction of the Stark level listed in the appendix. The principal magnetic susceptibilities $\chi_\parallel$ and $\chi_\perp$, and the anisotropy $\Delta\chi = \chi_\perp - \chi_\parallel$ are obtained from equation (9). The effective magnetic dipole moment $\mu_{eff} = (3kT\bar{\chi}/N)^{1/2}$, where $\bar{\chi} = (\chi_\parallel + 2\chi_\perp)/3$ is the mean mole magnetic susceptibility. In Tm^{3+}:$LiYF_4$, the first excited multiplet of the Tm^{3+} ion, $^3F_4$, is higher by 5500 cm^{-1} than the ground term $^3H_6$.

Hence the CF effect of the excited terms on the ground term is neglected in the following calculation. On the basis of the perturbation technique and the group-chain scheme, E_i^1 and E_i^2 are computed, and they are shown in table 5. The temperature dependences of C_S, $\bar{\chi}T$, μ_{eff}, and $\Delta\chi$ are plotted in figures 1–3.

Table 5. The Zeeman splitting of the Stark sublevels of $^3H_6$ in Tm^{3+}:$LiYF_4$.

	Group attribute		$\chi_\parallel$		$\chi_\perp$	
$^3H_6$	Γ	E_i^0	E_i^1 (in μ_B)	E_i^2 (in 10^{15} μ_B^2)	E_i^1 (in μ_B)	E_i^2 (in 10^{15} μ_B^2)
(a)	4	−6	0	−0.0983	0	−3.8655
(b)	5	26	± 0.2739	−0.0648	0	0.0253
(c)	1	57	0	−0.0666	0	3.6630
(d)	3	273	0	−8.0260	0	−0.3720
(e)	4	298	0	7.7480	0	−0.3960
(f)	2	336	0	−1.5290	0	−4.2530
(g)	5	347	± 5.8248	−0.0077	0	1.8180
(h)	1	393	0	1.5960	0	12.2450
(i)	5	387	± 2.0514	0.0725	0	−7.3650
(j)	3	414	0	0.3760	0	4.0390

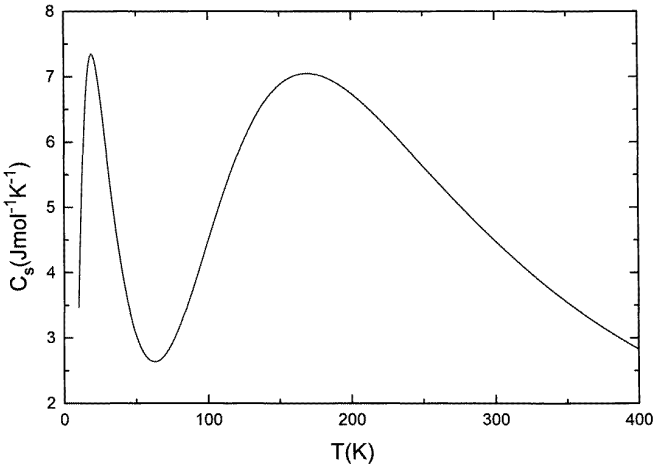

Figure 1. The temperature variation of the Schottky specific heat for Tm^{3+}:$LiYF_4$.

Figure 1 exhibits two peaks with the magnitudes 7.35 J mol^{-1} K^{-1} at 19 K and 7.05 J mol^{-1} K^{-1} at 170 K respectively. The appearance of a comparatively broad peak at 170 K is due to the fact that the fourth Stark level is separated from the third by 216 cm^{-1}, which is much larger than the CF splittings of 63 cm^{-1} and 141 cm^{-1} of the two groups so formed. The small CF splittings (63 cm^{-1}) should contribute to the appearance of the peak at low temperature. The extra entropy associated with the Schottky anomaly estimated from the specific heat curve up to 400 K is 18.94 J mol^{-1} K^{-1}. This value agrees fairly well with the free-ion value (21.31) obtained from the entropy expression for a system with a singlet ground state, $S = R\ln(2J + 1)$.

From figures 2 and 3, it is evident that $\chi_\parallel$ is always less than $\chi_\perp$. The values of $\bar{\chi}T$ and μ_{eff} do not change by more than 10% and 5% from 90 K to 400 K. The effective

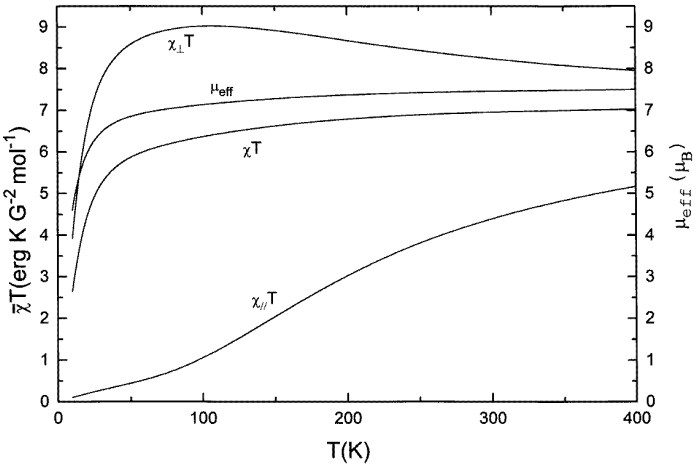

Figure 2. The temperature variation of the principal susceptibilities for Tm^{3+}:$LiYF_4$.

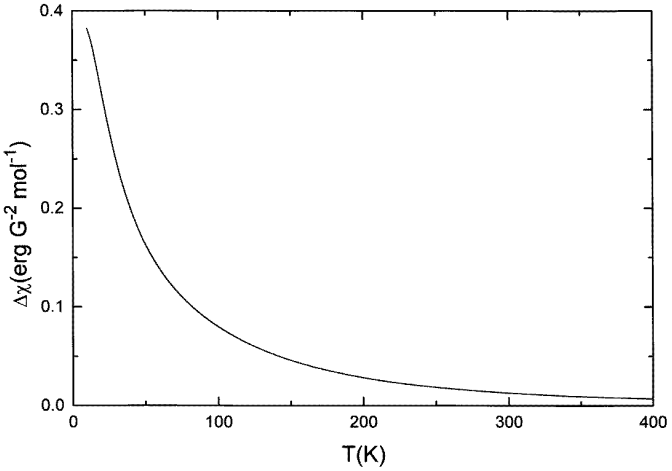

Figure 3. The temperature variation of the magnetic anisotropy for Tm^{3+}:$LiYF_4$.

magnetic moment at room temperature turns out to be 7.464 μ_B, which agrees well with the free-ion magnitude 7.56 μ_B for the Tm^{3+} ion obtained from Hund's formula, as well as the experimental value 7.61 μ_B for Tm metal [16]. Its deviation is the result of the large CF splitting of 420 cm^{-1} of the $^3H_6$ ground term. The mean magnetic susceptibility for temperatures above 100 K is fitted by the Curie–Weiss law $\bar{\chi} = C/(T + \theta)$. Finally the Curie constant (C) and Curie temperature (θ) turn out to be 7.26 erg K G^{-2} mol^{-1} and 13.44 K respectively. The magnetic anisotropy $\Delta\chi$ increases sharply with the fall of the temperature, which is in accordance with the low symmetry of the CF in Tm^{3+}:$LiYF_4$.

It is exciting for us to find that the curves depicted here are in good agreement with those of Kumar *et al* [3], in spite of the different methods adopted in the two calculations. Therefore it is reasonable to conclude that the method introduced in this paper is effective, and that the CF parameters are reliable.

5. Study of the polarization and relative intensities of emissions

JO theory [17, 18] demonstrates that the k-odd CF parameters, via configuration admixing, allow the occurrence of electric dipole transitions within $4f^n$ configurations. As for the Tm^{3+} ion in $LiYF_4$ crystal, supposing that Tm^{3+} ions occupy the D_{2d} sites, the odd-parity Hamiltonian can be expressed as

$$H_{cf} = C^{3^-}_{\tilde{0}^-00} b^{3^-}_{\tilde{0}^-00} + C^{5^-}_{2^-20} b^{5^-}_{2^-20} + C^{7^-}_{\tilde{0}^-00} b^{7^-}_{\tilde{0}^-00} + C^{7^-}_{2^-20} b^{7^-}_{2^-20}. \tag{12}$$

The electric dipole moment operators are given by

$$P_{\xi\beta} = -e \sum_i (b^{1^-}_{1^-\tilde{1}\xi\beta})_i r_i \tag{13}$$

where 1^-, 1^-, $\tilde{1}$ and ξ are irreducible representations of the group chain $O_3 \supset O_h \supset T_d \supset D_{2d}$; β is the projection of the ξ-representation; and $P_{\xi\beta}$ has three components corresponding to one π- and two σ-polarization spectra respectively. On the basis of the wavefunctions obtained, we can calculate the line-to-line intensities quantitatively for the emissions from $^1D_2$. The calculation is just the same as that of Nd^{3+}:YVO_4 [9] except that the programmes adopted in this paper take into account the effect of $4f^{N-1}5g$ configurations or seventh-order odd CF. The details of the effects of $4f^{N-1}ng$ configurations are discussed in [19]. We would like to present the final results here.

The transition matrix element connecting initial and final states can be written as

$$\begin{aligned}
&\langle f^n SLJ a_1 a_2 a_3 \alpha | P_{\xi\beta} | f^n S'L'J' d_1 d_2 d_3 \gamma \rangle \\
&= -2e \sum_{k c_1 c_2} \frac{A^k_{c_1 c_2}}{\Delta(nl)} \sum_{\lambda e_1 e_2 e_3 S S_1 S_2 S_3} (-1)^{k-\lambda-1} (2\lambda+1) \begin{pmatrix} \lambda \\ e_1 \end{pmatrix} \begin{matrix} O_3 \\ O_h \end{matrix} \begin{pmatrix} e_1 \\ e_2 \end{pmatrix} \begin{matrix} O_h \\ T_d \end{matrix} \\
&\times \begin{pmatrix} e_2 \\ e_3 \end{pmatrix} \begin{matrix} T_d \\ D_{2d} \end{matrix} \begin{pmatrix} e_3 \\ \mu \end{pmatrix} \begin{matrix} D_{2d} \\ S_4 \end{matrix} \begin{pmatrix} 1^- & k & \lambda^* \\ 1^- & c_1 & e_1^* \end{pmatrix} \begin{matrix} O_3 & s \\ O_h & s_1 \end{matrix} \begin{pmatrix} 1^- & c_1 & e_1^* \\ \tilde{1} & c_2 & e_2^* \end{pmatrix} \begin{matrix} O_h & s_1 \\ T_d & s_2 \end{matrix} \\
&\times \begin{pmatrix} \tilde{1} & c_2 & e_2^* \\ \xi & 0 & e_3^* \end{pmatrix} \begin{matrix} T_d & s_2 \\ D_{2d} & s_3 \end{matrix} \begin{pmatrix} \xi & 0 & e_3^* \\ \beta & 0 & \mu \end{pmatrix} \begin{matrix} D_{2d} & s_3 \\ S_4 & \end{matrix} (-1)^\lambda \langle nl|r|n'l' \rangle \\
&\times \langle nl|r^k|n'l' \rangle \begin{Bmatrix} 1 & k & \lambda \\ l & l & l' \end{Bmatrix} \langle nl||C^{(1)}||n'l' \rangle \langle n'l'||C^{(k)}||nl \rangle \begin{pmatrix} J \\ a_1 \end{pmatrix} \begin{matrix} O_3 \\ O_h \end{matrix} \\
&\times \begin{pmatrix} a_1 \\ a_2 \end{pmatrix} \begin{matrix} O_h \\ T_d \end{matrix} \begin{pmatrix} a_2 \\ a_3 \end{pmatrix} \begin{matrix} T_d \\ D_{2d} \end{matrix} \begin{pmatrix} a_3 \\ \alpha \end{pmatrix} \begin{matrix} D_{2d} \\ S_4 \end{matrix} \sum_{r r_1 r_2 r_3} \begin{pmatrix} J^* & \lambda & J' \\ a_1^* & e_1 & d_1 \end{pmatrix} \begin{matrix} O_3 & r \\ O_h & r_1 \end{matrix} \\
&\times \begin{pmatrix} a_1^* & e_1 & d_1 \\ a_2^* & e_2 & d_2 \end{pmatrix} \begin{matrix} O_h & r_1 \\ T_d & r_2 \end{matrix} \begin{pmatrix} a_2^* & e_2 & d_2 \\ a_3^* & e_3 & d_3 \end{pmatrix} \begin{matrix} T_d & r_2 \\ D_{2d} & r_3 \end{matrix} \\
&\times \begin{pmatrix} a_3^* & e_3 & d_3 \\ \alpha^* & \mu & \gamma \end{pmatrix} \begin{matrix} D_{2d} & r_3 \\ S_4 & \end{matrix} \langle f^n SLJ||U^{(\lambda)}||f^n S'L'J' \rangle
\end{aligned} \tag{14}$$

where

$$\Delta(nl') = \begin{cases} \Delta(5d) & k = 3, 5 \\ \Delta(5g) & k = 7. \end{cases}$$

$\Delta(nl')$ is the energy separation between the initial (or final) states and the intermediate states belonging to the configuration with different parity. All other symbols have the same physical meanings as in [9]. Note that there are a few mistakes in the expression given for the transition matrix element in [9]. The corrected result has been given as equation (14). To calculate the intensities for the transitions from the sublevels of the $^1D_2$ manifold to those lower manifolds, the Boltzmann distribution factor $\exp(-\Delta E/kT)$

describing the distribution of the particle number among all of the sublevels of $^1D_2$ should be considered. These factors, for four sublevels of $^1D_2$, are 1, 0.5624, 0.1712, and 0.1123 at 75 K respectively, in which the unit is set as that of the lowest sublevel. The relations between the transition rate, line strength, and fluorescence branching ratio are as follows:

$$A(\alpha J, \alpha' J') = \left[64\pi^4 f^3 e^2/3h(2J+1)\right] N S_{JJ'} \tag{15}$$

$$S_{JJ'} = (1/e^2) \sum_{i,f} \langle \Psi_{Ji} | P_{\xi\beta} | \Psi_{J'f} \rangle^2 \tag{16}$$

$$\beta(\alpha J, \alpha' J') = A(\alpha J, \alpha' J') \Big/ \sum_{\alpha' J'} A(\alpha J, \alpha' J') \tag{17}$$

where $N = (N_\pi + 2N_\sigma)/3$, $N_{\sigma,\pi} = n_{\sigma,\pi}(n_{\sigma,\pi}^2 + 2)^2/9$.

The experimental values of the branching ratios and the refractive index, and related spectroscopic data are compared to those from [2, 20] and listed in table 6.

Table 6. Spectroscopic experimental results for the Tm^{3+}:$LiYF_4$ crystal.

Transition from $^1D_2$	f (cm^{-1})	n_π	n_σ	β (from [2])	β (present fit)
$^1D_2 \rightarrow {}^3H_6$	27 774	1.4900	1.4667	56.64%	56.63%
$^1D_2 \rightarrow {}^3F_4$	22 188	1.4821	1.4591	29.27%	29.29%
$^1D_2 \rightarrow {}^3H_5$	19 585	1.4791	1.4561	0.35%	0.43%
$^1D_2 \rightarrow {}^3H_4$	15 291	1.4746	1.4527	5.63%	5.61%
$^1D_2 \rightarrow {}^3F_3$	13 460	1.4734	1.4509	3.45%	3.29%
$^1D_2 \rightarrow {}^3F_2$	12 825	1.4727	1.4503	3.90%	3.69%
$^1D_2 \rightarrow {}^1G_4$	6687	1.4674	1.4455	0.67%	0.39%

Table 7. Calculated relative line strengths and polarizations for all of the sublevels of $^1D_2$ and $^3F_4$ in Tm^{3+}:$LiYF_4$ at 75 K.

	The upper level of $^1D_2$			
The lower level of $^3H_6$	Γ_4(a)	Γ_3(b)	Γ_5(c)	Γ_1(d)
Γ_1(a)	81π (447.2 nm)	52π (449.7 nm)	2σ (445.4 nm)	—
Γ_2(b)	—	3σ (449.8 nm)	0.2σ (448.5 nm)	—
Γ_5(c)	100σ (450.4 nm)	—	5π (448.5 nm)	9σ (448.1 nm)
Γ_4(d)	—	—	16σ (449.8 nm)	3π (449.3 nm)
Γ_3(e)	—	—	7σ (452.3 nm)	—
Γ_1(f)	6π (454.7 nm)	—	11σ (452.8 nm)	—
Γ_5(g)	30σ (454.8 nm)	26σ (454.2 nm)	1π (452.9 nm)	2σ (452.4 nm)

By performing a least-squares fit to the branching ratios of $^1D_2$, the odd CF parameters $A^k_{c_1c_2}$ can be obtained: $A^{3^-}_{\tilde{0}^-0} = 6.2038A^{1/2}$, $A^{5^-}_{2^-2} = 3.5241A^{1/2}$, $A^{7^-}_{\tilde{0}^-0} = 13.4279A^{1/2}$, $A^{7^-}_{2^-2} = 5.2735A^{1/2}$, where A is a factor proportional to the total transition intensities $\sum_{\alpha' J'} A(\alpha J, \alpha' J')$. The relative intensities and polarizations of the radiative transitions from the sublevels of $^1D_2$ can be estimated. In order to compare them with the experimental data from the laser output, we only need to list the results concerned with the transition $^1D_2 \rightarrow {}^3F_4$ (see table 7, where the strongest line is normalized to 100, and the wavelengths are included in parentheses). Although the constraint ratios are not considered in the fit, the ratio of the seventh-order CF parameters, namely $A^{7^-}_{2^-2}/A^{7^-}_{\tilde{0}^-0}$, takes the value 0.3928, which

agrees well with the value 0.4148 easily obtained from the lattice sum. The agreement indicates that the CF parameters obtained correspond to physical reality and so are reliable. As shown in table 7, the predicted polarization of the line obeys the selection rules for electric dipole transitions in D_{2d} symmetry. The strongest line $^1D_2\ \Gamma_4(a) \rightarrow {}^3F_4\ \Gamma_5(c)$ is σ-polarized at 450.4 nm, which compares well with the experimental results [4–7]. In reference [4], blue upconversion laser emission was observed at 450.2 nm with σ-polarization. The observed wavelength also corresponds to transitions from the lowest Γ_4 level of $^1D_2$ to the lowest Γ_5 level of $^3F_4$. The second-strongest line $^1D_2\ \Gamma_4(a) \rightarrow {}^3F_4\ \Gamma_1(a)$ is π-polarized at 447.2 nm, while the π-polarized upconversion laser was also realized at 450.2 nm. The shift of the wavelength may be due to the assignment of D_{2d} site symmetry to Tm^{3+}.

6. Conclusion

A group-chain scheme analysis has been carried out for Tm^{3+} ions of $LiYF_4$ at D_{2d} low-symmetry sites, and a CF energy-level fitting has been performed by using the constraint condition determined by the ratios of the same-order CF parameters calculated using a simple point-charge model. With the aid of least-squares fitting programmes, the CF parameters with real physical meaning and the wavefunctions of Stark sublevels belonging to 11 manifolds have been obtained. The RMS value of the fit is 11.4 cm^{-1}.

On the basis of the wavefunctions obtained, the g-factors of the excited states of the terms concerned are calculated, and they confirm the partial g-sum rule of Karayianis. Considering just the CF effect of the ground state $^3H_6$, the temperature dependence of the Schottky specific heat, the magnetic susceptibility, and the anisotropy are described and depicted for Tm^{3+}:$LiYF_4$ from 10 to 400 K. The agreement with the experimental and theoretical results published by others shows that the method proposed is effective, and that the CF parameters are reliable. When the group-chain scheme, JO theory, and the effects of the seventh-order odd CF are combined in the calculation, the relative line strengths and the polarizations of the emission spectra can be predicted theoretically. In this paper, interest is focused on the upconversion lasing $^1D_2 \rightarrow {}^3F_4$. The strongest line calculated is σ-polarized at 450.4 nm, which compares well with the experimental results for upconversion lasing.

In conclusion, we have studied the energy structures, and spectroscopic and magnetic properties of Tm^{3+}:$LiYF_4$ crystal using CF analysis. The method introduced is simple but useful in the investigation of new laser and magnetic materials.

Acknowledgment

This project was supported by the Fujian Provincial Science Foundation of China.

Appendix. Wavefunctions for the crystal-field energy levels in Tm^{3+}:$LiYF_4$ ($O_3 \supset O_h \supset T_d \supset D_{2d}$)

$^3H_6(a)$	$-0.2985\|6^+\tilde{1}_0^+\tilde{1}\tilde{2}\rangle + 0.9544\|6^+\tilde{1}_1^+\tilde{1}\tilde{2}\rangle$	(Γ_4)
$^3H_6(b)$	$0.7437\|6^+1^+11\rangle + 0.2147\|6^+\tilde{1}_0^+\tilde{1}1\rangle + 0.6331\|6^+\tilde{1}_1^+\tilde{1}1\rangle$	(Γ_5)
$^3H_6(c)$	$0.7079\|6^+0^+00\rangle - 0.7063\|6^+2^+20\rangle$	(Γ_1)
$^3H_6(d)$	$0.9736\|6^+2^+22\rangle - 0.2285\|6^+\tilde{0}^+\tilde{0}2\rangle$	(Γ_3)
$^3H_6(e)$	$0.9544\|6^+\tilde{1}_0^+\tilde{1}\tilde{2}\rangle + 0.2985\|6^+\tilde{1}_1^+\tilde{1}\tilde{2}\rangle$	(Γ_4)

$^3H_6(f)$	$\|6^+1^+1\tilde{0}\rangle$	(Γ_2)
$^3H_6(g)$	$-0.5720\|6^+1^+11\rangle - 0.2858\|6^+\tilde{1}_0^+\tilde{1}1\rangle + 0.7688\|6^+\tilde{1}_1^+\tilde{1}1\rangle$	(Γ_5)
$^3H_6(h)$	$0.7063\|6^+0^+00\rangle + 0.7079\|6^+2^+20\rangle$	(Γ_1)
$^3H_6(i)$	$-0.3460\|6^+1^+11\rangle + 0.9339\|6^+\tilde{1}_0^+\tilde{1}1\rangle + 0.0897\|6^+\tilde{1}_1^+\tilde{1}1\rangle$	(Γ_5)
$^3H_6(j)$	$0.2285\|6^+2^+22\rangle + 0.9736\|6^+\tilde{0}^+\tilde{0}2\rangle$	(Γ_3)
$^3F_4(a)$	$0.0712\|4^+0^+00\rangle + 0.9975\|4^+2^+20\rangle$	(Γ_1)
$^3F_4(b)$	$\|4^+1^+1\tilde{0}\rangle$	(Γ_2)
$^3F_4(c)$	$0.6098\|4^+1^+11\rangle + 0.7925\|4^+\tilde{1}^+\tilde{1}1\rangle$	(Γ_5)
$^3F_4(d)$	$\|4^+\tilde{1}^+\tilde{1}\tilde{2}\rangle$	(Γ_4)
$^3F_4(e)$	$\|4^+2^+22\rangle$	(Γ_3)
$^3F_4(f)$	$-0.9975\|4^+0^+00\rangle + 0.0712\|4^+2^+20\rangle$	(Γ_1)
$^3F_4(g)$	$-0.7925\|4^+1^+11\rangle + 0.6098\|4^+\tilde{1}^+\tilde{1}1\rangle$	(Γ_5)
$^3H_5(a)$	$\|5^+2^+22\rangle$	(Γ_3)
$^3H_5(b)$	$-0.7137\|5^+1^+11\rangle + 0.5492\|5^+\tilde{1}_0^+\tilde{1}1\rangle - 0.4346\|5^+\tilde{1}_1^+\tilde{1}1\rangle$	(Γ_5)
$^3H_5(c)$	$-0.7127\|5^+1_0^+1\tilde{0}\rangle - 0.7015\|5^+1_1^+1\tilde{0}\rangle$	(Γ_2)
$^3H_5(d)$	$-0.1229\|5^+1^+11\rangle - 0.7091\|5^+\tilde{1}_0^+\tilde{1}1\rangle - 0.6943\|5^+\tilde{1}_1^+\tilde{1}1\rangle$	(Γ_5)
$^3H_5(e)$	$\|5^+2^+20\rangle$	(Γ_1)
$^3H_5(f)$	$\|5^+\tilde{1}^+\tilde{1}\tilde{2}\rangle$	(Γ_4)
$^3H_5(g)$	$-0.6895\|5^+1^+11\rangle - 0.4421\|5^+\tilde{1}_0^+\tilde{1}1\rangle + 0.5736\|5^+\tilde{1}_1^+\tilde{1}1\rangle$	(Γ_5)
$^3H_5(h)$	$-0.7015\|5^+1_0^+1\tilde{0}\rangle + 0.7127\|5^+1_1^+1\tilde{0}\rangle$	(Γ_2)
$^3H_4(a)$	$\|4^+\tilde{1}^+\tilde{1}\tilde{2}\rangle$	(Γ_4)
$^3H_4(b)$	$-0.9766\|4^+0^+00\rangle - 0.2152\|4^+2^+20\rangle$	(Γ_1)
$^3H_4(c)$	$0.6443\|4^+1^+11\rangle + 0.7648\|4^+\tilde{1}^+\tilde{1}1\rangle$	(Γ_5)
$^3H_4(d)$	$\|4^+1^+1\tilde{0}\rangle$	(Γ_2)
$^3H_4(e)$	$-0.2152\|4^+0^+00\rangle + 0.9766\|4^+2^+20\rangle$	(Γ_1)
$^3H_4(f)$	$-0.7648\|4^+1^+11\rangle + 0.6443\|4^+\tilde{1}^+\tilde{1}1\rangle$	(Γ_5)
$^3H_4(g)$	$\|4^+2^+22\rangle$	(Γ_3)
$^3F_3(a)$	$-0.3875\|3^+1^+11\rangle + 0.9219\|3^+\tilde{1}^+\tilde{1}1\rangle$	(Γ_5)
$^3F_3(b)$	$\|3^+\tilde{1}^+\tilde{1}\tilde{2}\rangle$	(Γ_4)
$^3F_3(c)$	$0.9219\|3^+1^+11\rangle + 0.3875\|3^+\tilde{1}^+\tilde{1}1\rangle$	(Γ_5)
$^3F_3(d)$	$\|3^+\tilde{0}^+\tilde{0}2\rangle$	(Γ_3)
$^3F_3(e)$	$\|3^+1^+1\tilde{0}\rangle$	(Γ_2)
$^3F_2(a)$	$\|2^+2^+22\rangle$	(Γ_3)

$^3F_2$(b)	$\|2^+\tilde{1}^+\tilde{1}1\rangle$	(Γ_5)
$^3F_2$(c)	$\|2^+\tilde{1}^+\tilde{1}\tilde{2}\rangle$	(Γ_4)
$^3F_2$(d)	$\|2^+2^+20\rangle$	(Γ_1)
$^1G_4$(a)	$0.1533\|4^+0^+00\rangle + 0.9882\|4^+2^+20\rangle$	(Γ_1)
$^1G_4$(b)	$0.6537\|4^+1^+11\rangle + 0.7567\|4^+\tilde{1}^+\tilde{1}1\rangle$	(Γ_5)
$^1G_4$(c)	$\|4^+\tilde{1}^+\tilde{1}\tilde{2}\rangle$	(Γ_4)
$^1G_4$(d)	$\|4^+1^+1\tilde{0}\rangle$	(Γ_2)
$^1G_4$(e)	$\|4^+2^+22\rangle$	(Γ_3)
$^1G_4$(f)	$-0.7567\|4^+1^+11\rangle + 0.6537\|4^+\tilde{1}^+\tilde{1}1\rangle$	(Γ_5)
$^1G_4$(g)	$-0.9882\|4^+0^+00\rangle + 0.1533\|4^+2^+20\rangle$	(Γ_1)
$^1D_2$(a)	$\|2^+\tilde{1}^+\tilde{1}\tilde{2}\rangle$	(Γ_4)
$^1D_2$(b)	$\|2^+2^+22\rangle$	(Γ_3)
$^1D_2$(c)	$\|2^+\tilde{1}^+\tilde{1}1\rangle$	(Γ_5)
$^1D_2$(d)	$\|2^+2^+20\rangle$	(Γ_1)
$^1I_6$(a)	$0.5938\|6^+2^+22\rangle + 0.8046\|6^+\tilde{0}^+\tilde{0}2\rangle$	(Γ_3)
$^1I_6$(b)	$-0.3108\|6^+1^+11\rangle + 0.9064\|6^+\tilde{1}_0^+\tilde{1}1\rangle + 0.2861\|6^+\tilde{1}_1^+\tilde{1}1\rangle$	(Γ_5)
$^1I_6$(c)	$0.4657\|6^+0^+00\rangle + 0.8850\|6^+2^+20\rangle$	(Γ_1)
$^1I_6$(d)	$\|6^+1^+1\tilde{0}\rangle$	(Γ_2)
$^1I_6$(e)	$-0.0844\|6^+1^+11\rangle - 0.3261\|6^+\tilde{1}_0^+\tilde{1}1\rangle + 0.9416\|6^+\tilde{1}_1^+\tilde{1}1\rangle$	(Γ_5)
$^1I_6$(f)	$-0.3166\|6^+\tilde{1}_0^+\tilde{1}\tilde{2}\rangle + 0.9486\|6^+\tilde{1}_1^+\tilde{1}\tilde{2}\rangle$	(Γ_4)
$^1I_6$(g)	$-0.8850\|6^+0^+00\rangle + 0.4657\|6^+2^+20\rangle$	(Γ_1)
$^1I_6$(h)	$0.9467\|6^+1^+11\rangle + 0.2685\|6^+\tilde{1}_0^+\tilde{1}1\rangle + 0.1779\|6^+\tilde{1}_1^+\tilde{1}1\rangle$	(Γ_5)
$^1I_6$(i)	$-0.8046\|6^+2^+22\rangle + 0.5938\|6^+\tilde{0}^+\tilde{0}2\rangle$	(Γ_3)
$^1I_6$(j)	$0.9486\|6^+\tilde{1}_0^+\tilde{1}\tilde{2}\rangle + 0.3166\|6^+\tilde{1}_1^+\tilde{1}\tilde{2}\rangle$	(Γ_4)
$^3P_1$(a)	$\|1^+1^+1\tilde{0}\rangle$	(Γ_2)
$^3P_1$(b)	$\|1^+1^+11\rangle$	(Γ_5)
$^3P_2$(a)	$\|2^+2^+22\rangle$	(Γ_3)
$^3P_2$(b)	$\|2^+\tilde{1}^+\tilde{1}1\rangle$	(Γ_5)
$^3P_2$(c)	$\|2^+\tilde{1}^+\tilde{1}\tilde{2}\rangle$	(Γ_4)
$^3P_2$(d)	$\|2^+2^+20\rangle$	(Γ_1).

References

[1] Jenssen H P, Linz A, Leavitt R P, Morrison C A and Wortman D E 1975 *Phys. Rev.* B **11** 92
[2] Dulick M, Faulkner G E, Cockroft N J and Nguyen D C 1991 *J. Lumin.* **48+49** 512

[3] Kumar V, Vishwamittar and Chandra K 1977 *J. Phys. C: Solid State Phys.* **10** 267
[4] Herbert T, Wannemacher R, Macfarlane R M and Length W 1992 *Appl. Phys. Lett.* **60** 2592
[5] Nguyen D C, Faulkner G E and Dulick M 1989 *Appl. Opt.* **28** 3553
[6] Nguyen D C, Faulkner G E, Weber M E and Dulick M 1990 *Proc. SPIE* **1223** 54
[7] Francois V, Pellé F, Goldner P and Simkin D 1995 *J. Lumin.* **65** 57
[8] Luo Zundu and Huang Yidong 1993 *J. Phys.: Condens. Matter* **5** 6949
[9] Luo Zundu and Huang Yidong 1994 *J. Phys.: Condens. Matter* **6** 3737
[10] Chen Xueyuan and Luo Zundu 1996 *J. Phys.: Condens. Matter* **8** 2571
[11] Thoma R E, Weaver C F, Friedman H A, Insley H, Harris L A and Yakel H A 1961 *J. Phys. Chem.* **65** 1096
[12] Butler P H 1981 *Point Group Symmetry Application: Method and Tables* (New York: Plenum)
[13] Pappalardo R 1976 *J. Lumin.* **14** 159
[14] Morrison C A and Leavitt R P 1979 *J. Chem. Phys.* **71** 2366
[15] Karayianis N 1971 *J. Chem. Phys.* **55** 3734
[16] Richards D B and Legvold S 1969 *Phys. Rev.* **186** 508
[17] Judd B R 1962 *Phys. Rev.* **127** 750
[18] Ofelt G S 1962 *J. Chem. Phys.* **37** 511
[19] Chen Xueyuan and Luo Zundu 1997 *Acta Phys. Sinica* (Chinese edition) **46** 183
[20] Castleberry D E and Linz A 1975 *Appl. Opt.* **14** 2056